# Optimal Parameter Extraction and Uncertainty Estimation in Intrinsic FET Small-Signal Models

Christian Fager, *Student Member, IEEE*, L. J. Peter Linnér, *Senior Member, IEEE*, and José Carlos Pedro, *Senior Member, IEEE*

***Abstract*—Analytical expressions for the relative sensitivities in the parameters of a standard intrinsic FET small-signal model with respect to deviations in the measured $S$-parameters are derived. This enables, in combination with a measurement uncertainty model, the model parameter uncertainties to be studied versus frequency. As a result, optimal, minimum uncertainty, parameter extraction can be performed independent of the bias voltage and without prior knowledge about the device frequency behavior, thus making it suitable for implementation in automatic multibias extraction programs.**

**The derived sensitivities are furthermore used to analytically calculate the uncertainty in the $S$-parameter response of the extracted model in terms of the uncertainties in either the parameters or the measurement it was extracted from.**

***Index Terms*—FET, measurement errors, modeling, parameter estimation, sensitivity, uncertainty, yield estimation.**

## I. Introduction

FOR MESFETs and high electron-mobility transistors (HEMTs), the procedure of extracting small-signal model parameters is well established. Usually direct-extraction methods are used [1]–[4].

During the extraction process the measurement uncertainties will give rise to corresponding uncertainties in the model parameters. The measurement uncertainties arise from limited dynamic range and accuracy of the measurement equipment, calibration-standard accuracy and repeatability problems, etc.

Nevertheless, little work has been reported on how to find the uncertainties with which the model parameters can be extracted.

In [5], King *et al.* give quantitative figures for the uncertainty of intrinsic FET model parameters. Analytical expressions have been used, but since only numerical figures are given at a single frequency and bias point, it is difficult to draw any general conclusions from those results.

Walters *et al.* present in [6] experimental results for measurement uncertainties and the resulting uncertainty in extracted small-signal parameters. No details are given about the derivation of the model parameter uncertainties.

Manuscript received April 5, 2002; revised August 25, 2002. This work was supported by the Swedish Foundation for Strategic Research (e-mail: fager@ep.chalmers.se).

C. Fager and L. J. P. Linnér are with the Microwave Electronics Laboratory, Chalmers University of Technology, 412 96 Gothenburg, Sweden.

J. C. Pedro is with the Instituto de Telecomunicações, University of Aveiro, 3810-193 Aveiro, Portugal

Digital Object Identifier 10.1109/TMTT.2002.805185

In this paper, the intrinsic model parameter uncertainties are analytically related to the $S$-parameter measurement uncertainties using a sensitivity analysis. The model parameter uncertainties are used to perform optimal, minimum uncertainty, parameter extraction without having prior knowledge about the device frequency characteristics.

Also, the derived sensitivities are used in the opposite direction, i.e., to relate the uncertainty in the modeled $S$-parameter response to either the model parameter uncertainties or to the uncertainty in the measurement it was originally extracted from. This gives information that, for example, can be used for design yield estimation, which normally would require a separate sensitivity analysis [7], [8] or a Monte Carlo simulation [9].

## II. Sensitivities and Uncertainty Estimation

The relative sensitivity,[1] $K$, in a parameter $x$ for relative changes in, e.g., $S_{11}$ is defined as

$$K_{S_{11}}^{x} \triangleq \frac{\frac{\partial x}{x}}{\frac{\partial S_{11}}{S_{11}}} = \frac{\partial x}{\partial S_{11}} \frac{S_{11}}{x}. \tag{1}$$

If $x$ only depends on $S_{11}$, the relative change in $x$ can be related to the relative change in $S_{11}$ using the sensitivity in (1)

$$\frac{\Delta x}{x} \cong K_{S_{11}}^{x} \frac{\Delta S_{11}}{S_{11}}. \tag{2}$$

In an FET modeling context the sensitivities may typically be used to calculate a relative change in the transconductance for a relative change in the measured magnitude of $S_{21}$.

Usually, the model parameters depend on all measured $S$-parameters. Thus, when calculating the change in $x$, the contributions from all $S$-parameters must be considered and added. The change in $x$ can then be expressed in a compact form as

$$\frac{\Delta x}{x} \cong \sum_{\forall k,l \in \{1,2\}} K_{S_{kl}}^{x} \frac{\Delta S_{kl}}{S_{kl}}. \tag{3}$$

In fact, this represents a first-order Taylor series expansion of $x$ in terms of the complex $S$-parameters. It is, therefore, valid only as long as the $\Delta S_{kl}$ are sufficiently small. For larger $\Delta S_{kl}$, higher order derivatives/sensitivities must be taken into account. However, for most parameters, the first order approximation is good enough considering the relatively high accuracy obtained

[1]The notation $K$ is used instead of $S$ for the relative sensitivities to avoid confusion with the $S$-parameters.

TABLE I
EXTRINSIC $Y$-PARAMETER SENSITIVITIES

| $\mathrm{K}_S^{Y_e}$ | $S_{11}$ | $S_{12}$ | $S_{21}$ | $S_{22}$ |
|---|---|---|---|---|
| $Y_{e,11}$ | $\frac{2S_{11}(1+S_{22})^2}{\Delta_1\Delta_3}$ | $-\frac{2S_{12}S_{21}(1+S_{22})}{\Delta_1\Delta_3}$ | $-\frac{2S_{12}S_{21}(1+S_{22})}{\Delta_1\Delta_3}$ | $\frac{2S_{12}S_{21}S_{22}}{\Delta_1\Delta_3}$ |
| $Y_{e,12}$ | $-\frac{S_{11}(1+S_{22})}{\Delta_3}$ | $\frac{(1+S_{11})(1+S_{22})}{\Delta_3}$ | $\frac{2S_{12}S_{21}}{\Delta_3}$ | $-\frac{(1+S_{11})S_{22}}{\Delta_3}$ |
| $Y_{e,21}$ | $-\frac{S_{11}(1+S_{22})}{\Delta_3}$ | $\frac{2S_{12}S_{21}}{\Delta_3}$ | $\frac{(1+S_{11})(1+S_{22})}{\Delta_3}$ | $-\frac{(1+S_{11})S_{22}}{\Delta_3}$ |
| $Y_{e,22}$ | $\frac{2S_{11}S_{12}S_{21}}{\Delta_2\Delta_3}$ | $-\frac{2(1+S_{11})S_{12}S_{21}}{\Delta_2\Delta_3}$ | $-\frac{2(1+S_{11})S_{12}S_{21}}{\Delta_2\Delta_3}$ | $\frac{2(1+S_{11})^2S_{22}}{\Delta_2\Delta_3}$ |

in $S$-parameter measurements. Hereafter, the approximation in (3) is considered valid with equal sign used.

The measured $S$-parameters are complex variables. Thus, uncertainties may be expressed in terms of magnitude and phase deviations. Since every contribution must be added in the sensitivity calculations, the deviation in $x$ will be expressed in the measured $S$-parameters as

$$\frac{\Delta x}{x} = \sum_{\forall k,l\in\{1,2\}} K^x_{|S_{kl}|}\frac{\Delta|S_{kl}|}{|S_{kl}|} + K^x_{\angle S_{kl}}\Delta\angle S_{kl} \tag{4}$$

where it has been used that the magnitude and phase deviations are usually specified in relative and absolute terms, respectively.

Usually, more than one parameter is extracted from the $S$-parameters. The deviation in each of the model parameters can be expressed in the $S$-parameters deviations using sensitivities as shown in (4). All model parameter deviations can, therefore, be collected in a single matrix equation

$$\begin{bmatrix} \frac{\Delta x_1}{x_1} \\ \vdots \\ \frac{\Delta x_n}{x_n} \end{bmatrix} = \begin{bmatrix} K^{x_1}_{|S_{11}|} & \cdots & K^{x_1}_{\angle S_{22}} \\ \vdots & \ddots & \vdots \\ K^{x_n}_{|S_{11}|} & \cdots & K^{x_n}_{\angle S_{22}} \end{bmatrix} \begin{bmatrix} \frac{\Delta|S_{11}|}{\Delta|S_{11}|} \\ \vdots \\ \Delta\angle S_{22} \end{bmatrix} \tag{5}$$

or, simply,

$$\Delta\mathbf{x} = \mathbf{K}^{\mathbf{x}}_{\mathbf{S}}\Delta\mathbf{S} \tag{6}$$

where $\Delta\mathbf{x}$ and $\Delta\mathbf{S}$ contains the *relative*[2] model- and $S$-parameter deviations, respectively (phase being in fact a relative measure of the arc length to the radius). With the absolute phase deviations given in radians, it may be shown that the real magnitude and phase sensitivities are found from the same complex sensitivities in (3)

$$K^x_{|S_{kl}|} = \mathrm{Re}(K^x_{S_{kl}}) \tag{7}$$
$$K^x_{\angle S_{kl}} = -\mathrm{Im}(K^x_{S_{kl}}). \tag{8}$$

The measurement uncertainties are characterized by their statistical properties. If the $S$-parameter deviations are assumed to be normal-distributed having a zero mean and being uncorrelated makes it possible to use (6) to express the variances in $\mathbf{x}$ in terms of the $S$-parameter variances

$$\sigma^2_{\mathbf{x}} = (\mathbf{K}^{\mathbf{x}}_{\mathbf{S}})^2\sigma^2_{\mathbf{S}} \tag{9}$$

where $(\mathbf{K})^2$ denotes taking the square of each individual element in $\mathbf{K}$ and

$$\sigma^2_{\mathbf{x}} = [\sigma^2_{x_1} \quad \cdots \quad \sigma^2_{x_n}]^T \tag{10}$$
$$\sigma^2_{\mathbf{S}} = [\sigma^2_{|S_{11}|} \quad \sigma^2_{\angle S_{11}} \quad \cdots \quad \sigma^2_{|S_{22}|} \quad \sigma^2_{\angle S_{22}}]^T. \tag{11}$$

## III. PARAMETER SENSITIVITY CALCULATIONS

The uncertainties in the measured $S$-parameters will propagate to the model parameters in the same way as the model parameters are extracted. Hence, the sensitivity analysis may be carried out in parallel with the small-signal parameter extraction to find their uncertainties.

In the extraction of most small-signal models, the first step is to convert the measured $S$-parameters into extrinsic $Y$-parameters, e.g., by [10],

$$Y_e = -\frac{1}{\Delta_3}\begin{bmatrix} \Delta_1 & 2S_{12} \\ 2S_{21} & \Delta_2 \end{bmatrix} \tag{12}$$

where

$$\Delta_1 = (S_{11}-1)(S_{22}+1) - S_{12}S_{21} \tag{13}$$
$$\Delta_2 = (S_{11}+1)(S_{22}-1) - S_{12}S_{21} \tag{14}$$
$$\Delta_3 = (S_{11}+1)(S_{22}+1) - S_{12}S_{21}. \tag{15}$$

It is then straightforward to derive all extrinsic $Y$-parameter sensitivities using the definition in (1). The resulting sensitivities are collected in Table I.

Usually, a parasitic network that accounts for pad-, package-, and access-line effects surrounds the intrinsic FET models [1], [3].

If the parasitic element values are known, e.g., from a cold-FET extraction, the intrinsic $Y$-parameters, $Y_i$, can be found using de-embedding techniques [1], [11].

In this paper, the parasitic element values are assumed to be known with high accuracy. The intrinsic $Y$-parameter sensitivities can then be derived from the extrinsic $Y$-parameter sensitivities. Our experience is, however, that the resulting differences between extrinsic and intrinsic sensitivities are small—especially if the influence of the device parasitic elements is small, such as in on-wafer measurements.

[2]Observe that in (6), and equations derived therefrom, the symbols $\mathbf{x}$ and $\mathbf{S}$ represent relative quantities.

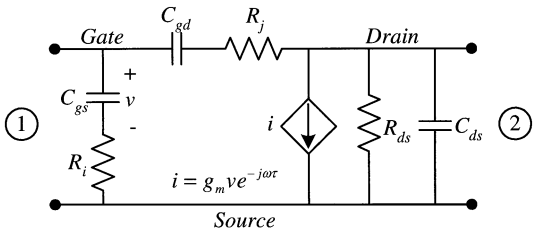


Fig. 1. High-frequency intrinsic FET small-signal model.

When the intrinsic $Y$-parameters are found, the model parameters are usually calculated analytically. Fig. 1 shows a commonly used intrinsic small-signal model shown to be valid up to very high frequencies [3].

The derivation of the model parameter sensitivities will be shown only for $C_{gs}$ and $R_i$, but is similar for the other parameters.

$C_{gs}$ and $R_i$ can be determined from the intrinsic admittance parameter $Y_{gs}$

$$Y_{gs} = Y_{i,11} + Y_{i,12} = \frac{j\omega C_{gs}}{1 + j\omega C_{gs} R_i}. \tag{16}$$

The relative sensitivity in $Y_{gs}$ can then be related to the $C_{gs}$ and $R_i$ sensitivities by

$$K_{S_{kl}}^{Y_{gs}} = \frac{\partial Y_{gs}}{\partial R_i} K_{S_{kl}}^{R_i} \frac{R_i}{Y_{gs}} + \frac{\partial Y_{gs}}{\partial C_{gs}} K_{S_{kl}}^{C_{gs}} \frac{C_{gs}}{Y_{gs}}. \tag{17}$$

Evaluating the partial derivatives yields after some simplifications

$$K_{S_{kl}}^{Y_{gs}} = -K_{S_{kl}}^{R_i} Y_{gs} R_i + \frac{Y_{gs} K_{S_{kl}}^{C_{gs}}}{j\omega C_{gs}}. \tag{18}$$

Since the sensitivities in the real model parameters, $C_{gs}$ and $R_i$, also must be real, their sensitivities can be identified from the real and imaginary parts of (18)

$$K_{S_{kl}}^{R_i} = \frac{\mathrm{Re}\left(-\frac{K_{S_{kl}}^{Y_{gs}}}{Y_{gs}}\right)}{R_i} \tag{19}$$

$$K_{S_{kl}}^{C_{gs}} = \omega C_{gs} \mathrm{Im}\left(-\frac{K_{S_{kl}}^{Y_{gs}}}{Y_{gs}}\right). \tag{20}$$

The complete list of parameter sensitivities with respect to magnitude deviations is collected in Table II where the admittance parameters are defined as

$$Y_{gs} = Y_{i,11} + Y_{i,12} \tag{21}$$

$$Y_{ds} = Y_{i,22} + Y_{i,12} \tag{22}$$

$$Y_{gd} = -Y_{i,12} \tag{23}$$

$$Y_m = Y_{i,21} - Y_{i,12}. \tag{24}$$

The corresponding admittance parameter sensitivities are given by

$$K_{S_{kl}}^{Y_{gs}} = \frac{K_{S_{kl}}^{Y_{i,11}} Y_{i,11}}{Y_{gs}} + \frac{K_{S_{kl}}^{Y_{i,12}} Y_{i,12}}{Y_{gs}} \tag{25}$$

$$K_{S_{kl}}^{Y_{gd}} = K_{S_{kl}}^{Y_i,12} \tag{26}$$

$$K_{S_{kl}}^{Y_m} = \frac{K_{S_{kl}}^{Y_{i,21}} Y_{i,21}}{Y_m} - \frac{K_{S_{kl}}^{Y_{i,12}} Y_{i,12}}{Y_m} \tag{27}$$

$$K_{S_{kl}}^{Y_{ds}} = \frac{K_{S_{kl}}^{Y_{i,12}} Y_{i,12}}{Y_{ds}} + \frac{K_{S_{kl}}^{Y_{i,22}} Y_{i,22}}{Y_{ds}}. \tag{28}$$

TABLE II
INTRINSIC MODEL PARAMETER SENSITIVITIES

| Parameter, $x$ | Relative magnitude sensitivity, $\mathrm{K}_{\lvert S_{kl}\rvert}^{x}$ |
|---|---|
| $R_i$ | $\mathrm{Re}\left(-\mathrm{K}_{S_{kl}}^{Y_{gs}}/Y_{gs}\right)\Big/R_i$ |
| $C_{gs}$ | $\omega C_{gs}\,\mathrm{Im}\left(-\mathrm{K}_{S_{kl}}^{Y_{gs}}/Y_{gs}\right)$ |
| $R_j$ | $\mathrm{Re}\left(-\mathrm{K}_{S_{kl}}^{Y_{gd}}/Y_{gd}\right)\Big/R_j$ |
| $C_{gd}$ | $\omega C_{gd}\,\mathrm{Im}\left(-\mathrm{K}_{S_{kl}}^{Y_{gd}}/Y_{gd}\right)$ |
| $g_{ds}$ | $\mathrm{Re}\left(Y_{ds}\mathrm{K}_{S_{kl}}^{Y_{ds}}\right)\Big/g_{ds}$ |
| $C_{ds}$ | $\mathrm{Im}\left(Y_{ds}\mathrm{K}_{S_{kl}}^{Y_{ds}}\right)\Big/\omega C_{ds}$ |
| $g_m$ | $\mathrm{Re}\left(\mathrm{K}_{S_{kl}}^{Y_m} + R_i Y_{gs}\left(\mathrm{K}_{\lvert S_{kl}\rvert}^{R_i} + \mathrm{K}_{\lvert S_{kl}\rvert}^{C_{gs}}\right)\right)$ |
| $\tau$ | $-\mathrm{Im}\left(\mathrm{K}_{S_{kl}}^{Y_m} + R_i Y_{gs}\left(\mathrm{K}_{\lvert S_{kl}\rvert}^{R_i} + \mathrm{K}_{\lvert S_{kl}\rvert}^{C_{gs}}\right)\right)\Big/\omega\tau$ |

The absolute phase sensitivities are, as discussed in the previous section, found by multiplying the complex sensitivities $K_{S_{kl}}^{Y_{xx}}$ in Table II with the imaginary unit.

Once the parameter sensitivities are known, their uncertainties can be estimated in terms of the $S$-parameter uncertainties using (9).

## IV. MODEL PARAMETER UNCERTAINTY

Measurements on an HEMT device are used together with an $S$-parameter measurement uncertainty model to estimate the uncertainty in the extracted parameter values. The transistor used is made in OMMIC's D01PH GaAs process,[3] and was measured with a 50-GHz Agilent 8510C vector network analyzer (VNA) using coplanar probes. Measurements made in the saturated region, used for maximum gain, are used to demonstrate the uncertainty calculations.

The parasitic elements were initially determined with the cold-FET method [1], [3]. Two of the intrinsic model parameters, $g_m$ and $R_j$, are studied, where $g_m$ is normally easy to extract whereas $R_j$ has a significant contribution only at higher frequencies and therefore is more difficult to extract. The frequency dependence of these parameters is shown in Fig. 2.

As is apparent from Fig. 2, the relative variations in $R_j$ are much larger than those in $g_m$ making it difficult to decide which value is the best to use.

To perform the parameter uncertainty calculations versus frequency, the $S$-parameter uncertainties must also be known. The $S$-parameter uncertainties are mainly due to limited dynamic range and accuracy of the VNA and accuracy of the calibration standards used. Evaluation of the measurement uncertainty using verification standards has shown that the uncertainties achieved using a careful on-wafer thru-reflect line (TRL) calibration [12] are close to the ones specified for the VNA.

An empirical $S$-parameter uncertainty model has therefore been developed for the relative magnitude and absolute phase

[3]D01PH GaAs MMIC Process, OMMIC. Limeil-Brevannes, France

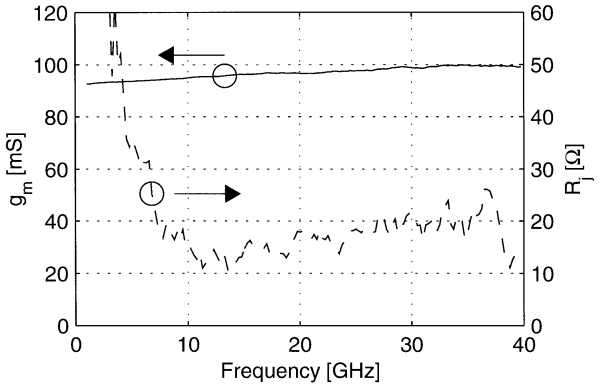


Fig. 2. Extracted $g_m$ and $R_j$ versus frequency.

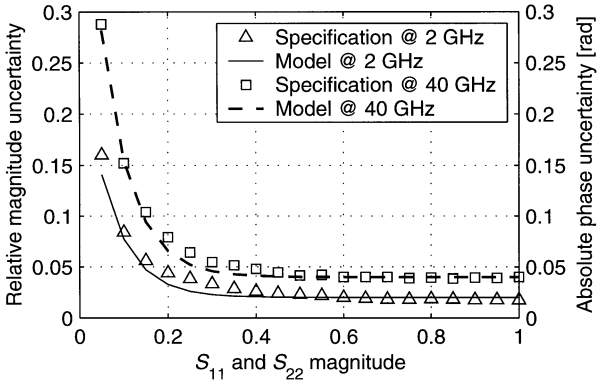


Fig. 3. Specified and modeled uncertainty in $S_{11}$ and $S_{22}$.

uncertainties from the VNA specifications [13]. The model used for $S_{11}$ and $S_{22}$ is given by

$$\sigma_{|S_{11,22}|} = \sigma_{\angle S_{11,22}} = \left(1 + e^{k_1(k_2 - |S_{11,22}|)}\right)(k_3 + k_4 f) \tag{29}$$

where $f$ is the frequency and $|S_{11,22}|$ the measured magnitude of $S_{11}$ and $S_{22}$, respectively, and $k_n$ are model parameters. The first factor accounts for the $S$-parameter magnitude dependence and the second factor the frequency dependence of the uncertainty. A similar model is used for the $S_{12}$ and $S_{21}$ uncertainties with $|S_{11,22}|$ replaced by $dB(|S_{12,21}|)$ in the model.

Note that the VNA specifications are given as *worst case*, which is usually taken as a $3\sigma$ confidence interval. $\sigma$ is in this text used as a general notation, hereafter in fact denoting $3\sigma$.

The model and specification is shown for $S_{11}$ and $S_{22}$ in Fig. 3. Note that the relative magnitude and absolute phase uncertainty specifications are coincident.

Using the uncertainty models together with the sensitivity expressions in Table II makes it possible to evaluate the uncertainty in the extracted model parameters for each measurement frequency and bias point of interest. Fig. 4 shows the calculated uncertainties for $g_m$, $R_j$, and $C_{gs}$ versus frequency in the same bias point as used before. From this figure it is clear that $g_m$ should be extracted at low frequencies while $R_j$ should be extracted at high frequencies where the parameter uncertainty is minimal. $C_{gs}$ has an intermediate optimal extraction frequency where the uncertainty is minimal. Table III shows all extracted

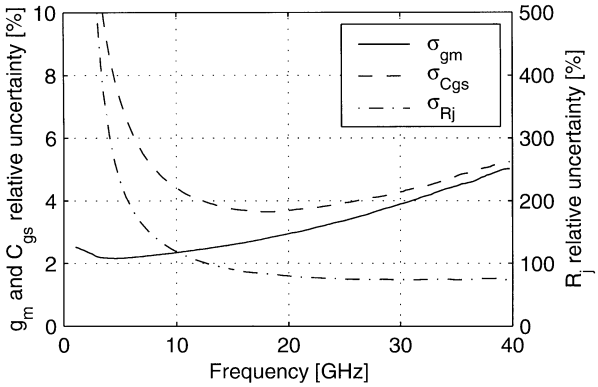


Fig. 4. Estimated relative uncertainty in $g_m$, $C_{gs}$, and $R_j$ versus frequency.

parameters with corresponding estimated uncertainties and their optimal extraction frequencies, $f_{opt}$. As can be seen in Table III, the uncertainty in $R_i$ prevents extraction of its value with any confidence.

Note that it may be necessary to perform a few iterations to find the minimum uncertainty frequencies since the sensitivity expressions—and, consequently, the parameter uncertainties—are expressed in terms of the sought parameter values.

In existing methods, constant extraction frequencies are set for the parameters independent of bias. Since the minimum uncertainty frequencies will vary with bias, the presented method gives inevitably more reliable multibias extraction results suitable for use in for example large-signal modeling.

Usually, to further reduce the parameter uncertainty, constant frequency ranges are set for each model parameter over which the parameters are averaged [14]. This results in a tradeoff between averaging range and parameter uncertainty and requires detailed knowledge about the frequency dependence of the model parameters for the device under test.

It is shown in the Appendix that, with knowledge of the parameter uncertainties, a weighted average can be calculated where more uncertain values are weighted less and vice versa in a way that the resulting uncertainty in the parameter estimation becomes minimal. Table III shows the optimally averaged parameter values, the frequency range they were extracted from and the resulting uncertainty.

Even if more uncertain values are automatically assigned less weight, care should be taken to avoid clearly erroneous values. This is easily done by, for example, only considering frequencies where $\sigma_x < 50\%$.

As for any method, accurate parameter extraction relies on accurate extraction of the parasitic elements and validity of the intrinsic model used. In this example, there is a slight slope of $g_m$ versus frequency making it difficult to tell which value is better (see Fig. 2). This is probably caused by a small error in the parasitic extraction. Averaging will then offset the value compared to the single frequency extraction in Table III. This problem is common to all direct-extraction methods, but is reduced using the presented weighted average where the more reliable values are pronounced. Nevertheless, the resulting parameter uncertainty may be underestimated in such cases.

TABLE III
EXTRACTED MODEL PARAMETERS WITH UNCERTAINTY ESTIMATION

| Parameter | Single frequency extraction | | | Weighted average extraction | | |
|---|---|---|---|---|---|---|
| | Value, $x$ | $\sigma_{x,min}$ [%] | $f_{opt}$ [GHz] | Value, $\bar{x}$ | $\sigma_{\bar{x}}$ [%] | $f_{min} - f_{max}$ |
| $R_i$ | 0.4 [Ω] | 380 | 40 | 0.4 [Ω] | 380 | 40 |
| $C_{gs}$ | 136 [fF] | 3.6 | 18 | 136 [fF] | 0.4 | 1 – 40 |
| $R_j$ | 14 [Ω] | 73 | 40 | 14 [Ω] | 73 | 40 |
| $C_{gd}$ | 14.8 [fF] | 1.4 | 6.3 | 14.7 [fF] | 0.2 | 1 – 40 |
| $g_{ds}$ | 4.8 [mS] | 5.6 | 1.0 | 4.75 [mS] | 0.6 | 1 – 40 |
| $C_{ds}$ | 26 [fF] | 8.3 | 37 | 25.2 [fF] | 0.9 | 4 – 40 |
| $g_m$ | 93.6 [mS] | 2.2 | 4.5 | 95.9 [mS] | 0.2 | 1 – 40 |
| $\tau$ | 0.38 [ps] | 39 | 40 | 0.36 [ps] | 5.8 | 27 – 40 |

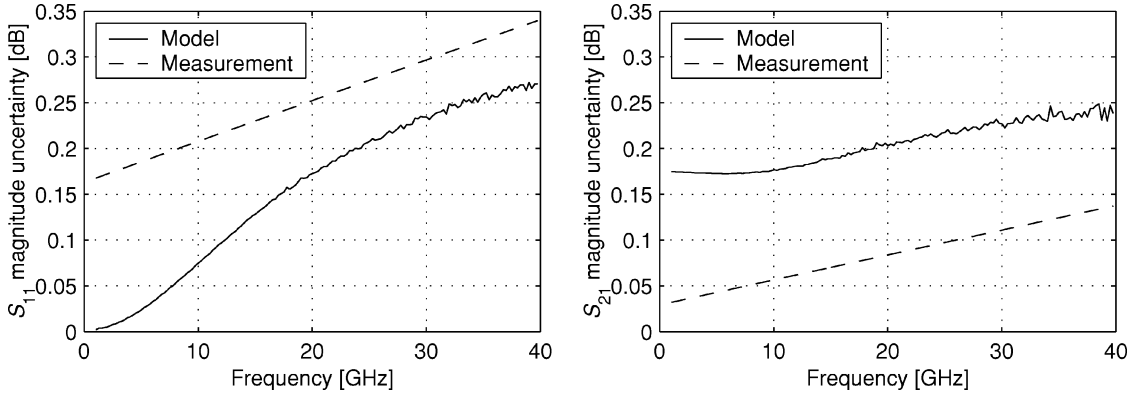


Fig. 5. Measurement uncertainty and model uncertainty for the magnitude of (a) $S_{11}$ and (b) $S_{21}$.

## V. MODEL RESPONSE UNCERTAINTY

The model parameter uncertainties, found in the previous section, result in a corresponding uncertainty in the $S$-parameter response when the model is used for simulation.

In (6), deviations in the model parameters are expressed as function of $S$-parameter deviations. If instead the model parameter deviations are given, the deviations in the $S$-parameters can be found from

$$\Delta \mathbf{S} = \mathbf{K}_{\mathbf{x}}^{\mathbf{S}} \Delta \mathbf{x} \tag{30}$$

where $\mathbf{K}_{\mathbf{x}}^{\mathbf{S}} = (\mathbf{K}_{\mathbf{S}}^{\mathbf{x}})^{-1}$. Hence, analogous to (9), the uncertainty in the simulated response is given by

$$\sigma_{\mathbf{S},sim}^2 = \left(\mathbf{K}_{\mathbf{x}}^{\mathbf{S}}\right)^2 \sigma_{\mathbf{x},\min}^2 \tag{31}$$

where $\sigma_{\mathbf{x},\min}^2$ is the previously calculated minimum variance in the extracted model parameters (see Table III). This expression can be combined with (9) to express the simulated response uncertainty directly in terms of the measured $S$-parameter uncertainties, which yields

$$\sigma_{\mathbf{S},sim}^2 = \left(\mathbf{K}_{\mathbf{x}}^{\mathbf{S}}\right)^2 \left(\mathbf{K}_{\mathbf{S},\min}^{\mathbf{x}}\right)^2 \sigma_{\mathbf{S},meas}^2. \tag{32}$$

As before, $(\mathbf{K})^2$ denotes element-wise squaring of the individual elements and $\mathbf{K}_{\mathbf{S},\min}^{\mathbf{x}}$ the model parameter sensitivities evaluated at the frequencies of least uncertainty.

In these calculations, it has been assumed that the extracted parameters are uncorrelated. This is valid if each of them is extracted at different frequencies, which may not be the case when averaging is applied.

The measurement uncertainty model and sensitivities used in the previous section have been applied in (32) to calculate the uncertainty in the response of the model. The single-frequency extraction in Table III has been used.

Fig. 5 shows the magnitude uncertainty in $S_{11}$ and $S_{21}$. It might seem counterintuitive that, for $|S_{11}|$, the response from the model gives lower uncertainty than the measurement it was extracted from. This is caused by the gate capacitances in the intrinsic model topology used (see Fig. 1), which forces the input to present $S_{11} \equiv 1$ at low frequency regardless of the measurement or any parameter value.

The magnitude of $S_{21}$, on the other hand, has no such restrictions and may take any value. The uncertainty in modeled $|S_{21}|$ will, therefore, inevitably be larger than in the measurement. Fig. 5 also shows that the gain of an amplifier design, using this model extraction, could not be specified within less than 0.2 dB.

## VI. CONCLUSIONS

An analytical derivation of the intrinsic FET model parameter sensitivities to variations in the extrinsic, measured, $S$-parameters was presented. Measurements on a commercial HEMT device have been used to illustrate how the sensitivity analysis, in combination with a measurement uncertainty model, can be used to calculate the uncertainty in the extracted small-signal model parameters. This makes optimal extraction of the model

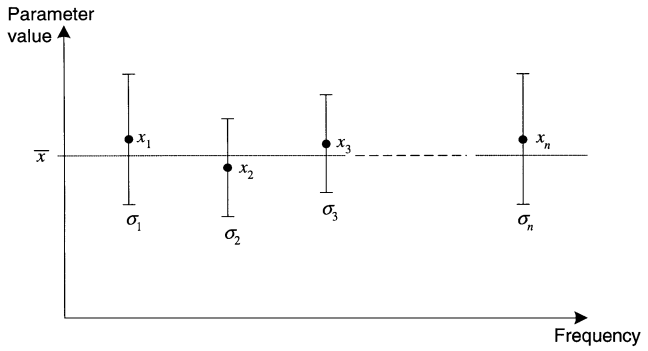


Fig. 6. Extracted parameter values with corresponding uncertainties versus frequency.

parameters possible without having any prior knowledge about the device frequency characteristics.

The resulting knowledge about the frequency dependence of the parameter uncertainties also enabled a "smart" averaging method to further minimize the parameter uncertainty.

The derived sensitivities have been used also in the opposite direction, i.e., to relate deviations in extrinsic $S$-parameters in terms of either the model parameter deviations or the $S$-parameter measurement it was based on. Thereby, it is possible to directly calculate the uncertainty in the modeled $S$-parameter response in terms of the uncertainty in the measurement it was extracted from.

Since the presented theory describes how optimal extraction of the small-signal FET model parameters can be performed independently at any bias voltage and without having any prior knowledge about the device frequency characteristics, we believe that it is well suited for implementation in multibias extraction software. Information about the uncertainties in extracted model parameters can, for example, be used to track the accuracy during extractions or to check the statistical significance of parameter variations in FET databases [15]. The calculated uncertainty in the model response gives information about the uncertainty in the circuit response, useful for design yield estimation, without any additional simulations being necessary.

## APPENDIX

In the presented analysis, the model parameter value and uncertainty can be found at each frequency as shown in Fig. 6.

A weighted average of the different parameter values can then be expressed as

$$\bar{x} = w_1 x_1 + w_2 x_2 + \cdots + w_n x_n \tag{A1}$$

$$\sum_{k=1}^{n} w_k = 1 \tag{A2}$$

where the weighting factors $w_k$ should be selected to minimize the variance in $\bar{x}$. Since it is assumed that the deviation at each measurement frequency is independent and normal-distributed, the variance in $\bar{x}$ can be expressed as

$$\sigma_{\bar{x}}^2 = w_1^2\sigma_1^2 + w_2^2\sigma_2^2 + \cdots + w_n^2\sigma_n^2 \tag{A3}$$

where $\sigma_k^2$ is the variance of the parameter at frequency $k$. For $\sigma_{\bar{x}}^2$ to be minimized, the partial derivatives with respect to each of the weighting factors should be zero

$$\frac{\partial \sigma_{\bar{x}}^2}{\partial w_k} = 2w_k\sigma_k^2 - 2\sigma_n^2\left(1 - \sum_{i=1}^{n-1} w_i\right) = 0 \tag{A4}$$

where (A2) has been used to eliminate the $n$th term in (A3). These equations can, after some manipulations, be arranged in a single matrix equation for the optimal weighting factors

$$\begin{bmatrix} \frac{\sigma_1^2}{\sigma_n^2} & 0 & \cdots & 0 & -1 \\ 0 & \frac{\sigma_2^2}{\sigma_n^2} & \cdots & 0 & -1 \\ \vdots & \vdots & \ddots & \vdots & \vdots \\ 0 & 0 & \cdots & \frac{\sigma_{n-1}^2}{\sigma_n^2} & -1 \\ 1 & 1 & \cdots & 1 & 1 \end{bmatrix} \begin{bmatrix} w_1 \\ w_2 \\ \vdots \\ w_{n-1} \\ w_n \end{bmatrix} = \begin{bmatrix} 0 \\ 0 \\ \vdots \\ 0 \\ 1 \end{bmatrix}. \tag{A5}$$

## ACKNOWLEDGMENT

The authors would like to thank Dr. M. Garcia, Raytheon, Andover, MA, and Dr. K. Yhland, Microwave Electronics Laboratory, Chalmers University of Technology, Göteborg, Sweden, for fruitful discussions.

## REFERENCES

[1] G. Dambrine, A. Cappy, F. Heliodore, and E. Playez, "A new method for determining the FET small-signal equivalent circuit," *IEEE Trans Microwave Theory Tech.*, vol. 36, pp. 1151–1159, July 1988.

[2] M. Berroth and R. Bosch, "Broad-band determination of the FET small-signal equivalent circuit," *IEEE Trans Microwave Theory Tech.*, vol. 38, pp. 891–895, July 1990.

[3] N. Rorsman, M. Garcia, C. Karlsson, and H. Zirath, "Accurate small-signal modeling of HFET's for millimeter-wave applications," *IEEE Trans Microwave Theory Tech.*, vol. 44, pp. 432–437, Mar. 1996.

[4] K. B. Sung, "Existence of optimum cold FET intrinsic reference plane for active FET small signal modeling," *IEEE Microwave Wireless Comp. Lett.*, vol. 11, pp. 302–304, July 2001.

[5] F. D. King, P. Winson, A. D. Snider, L. Dunleavy, and D. P. Levinson, "Math methods in transistor modeling: Condition numbers for parameter extraction," *IEEE Trans Microwave Theory Tech.*, vol. 46, pp. 1313–1314, Sept. 1998.

[6] P. Walters, R. Pollard, J. Richardson, P. Gamand, and P. Suchet, "On-wafer measurement uncertainty for 3-terminal active millimeter-wave devices," *GaAs IC Symp. Dig.*, pp. 55–58, 1992.

[7] J. W. Bandler, Z. Q. Jun, and R. M. Biernacki, "A unified theory for frequency-domain simulation and sensitivity analysis of linear and nonlinear circuits," *IEEE Trans Microwave Theory Tech.*, vol. 36, pp. 1661–1669, Dec. 1988.

[8] S. W. Director and R. A. Rohrer, "The generalized adjoint network and network sensitivities," *IEEE Trans Circuit Theory*, vol. 16, pp. 318–323, Aug. 1969.

[9] M. Meehan and J. Purviance, *Yield and Reliability Design for Microwave Circuits and Systems*. Norwood, MA: Artech House, 1993.

[10] L. J. P. Linnér, "Scattering parameters derived from the cofactors of the node admittance matrix," in *1987 IEEE Int. Symp. Circuits and Systems Dig.*, vol. 1, 1987, pp. 165–167.

[11] R. A. Pucel, W. Struble, R. Hallgren, and U. L. Rohde, "A general noise de-embedding procedure for packaged two-port linear active devices," *IEEE Trans Microwave Theory Tech.*, vol. 40, pp. 2013–2024, Nov. 1992.

[12] G. F. Engen and C. A. Hoer, "'Thru-reflect-line': An improved technique for calibrating the dual six-port automatic network analyzer," *IEEE Trans Microwave Theory and Tech.*, vol. 27, pp. 987–993, Dec. 1979.

[13] "8510C Network Analyzer Data Sheet," Agilent Technologies, Palo Alto, CA, 1999.

[14] M. Garcia, K. Yhland, H. Zirath, I. Angelov, and N. Rorsman, "Fast, automatic and accurate HFET small-signal characterization," *Microwave J.*, vol. 40, pp. 102–117, July 1997.

[15] J. Purviance, D. Criss, and D. Monteith, "FET model statistics and their effects on design centering and yield prediction for microwave amplifiers," in *1988 IEEE MTT Int. Microwave Symp. Dig*, vol. 1, 1988, pp. 315–318.

**Christian Fager** (S'98) was born in Varberg, Sweden, in 1974. He received the M.Sc. degree in electrical engineering in 1998 from Chalmers University of Technology, Gothenburg, Sweden, where he is currently working toward the Ph.D. degree in the Department of Microelectronics.

His research interests are in the areas of large-signal transistor modeling and nonlinear circuit design.

Mr. Fager received the Best Student Paper Award at the International Microwave Symposium in 2002.

**L. J. Peter Linnér** (S'68–M'74–SM'87) was born in Växjö, Sweden, in 1945. He received the M.Sc. and Ph.D. degrees in electrical engineering from Chalmers University of Technology, Gothenburg, Sweden, in 1969 and 1974, respectively.

In 1969, he became a Teaching Assistant in mathematics and telecommunications at Chalmers University of Technology. In 1973, he joined the research and teaching staff of the Division of Network Theory at the same university with research interests in the areas of network theory, microwave engineering, and computer-aided design methods. In 1974, he moved to the MI-division, Ericsson Telephone Company, Mölndal, Sweden, where he was a Systems Engineer and Project Leader for several military radar projects. He returned to Chalmers University of Technology as a Researcher in the areas of microwave array antenna systems. Since 1981, he has been an Associate Professor in telecommunications. For part of 1992, he was a Guest Researcher at the University of Bochum, Bochum, Germany. His current interest is in the application of computer-aided network methods in the area of microwave technology, as well as filter technology, in general.

**José Carlos Pedro** (S'90–M'95–SM'99) was born in Espinho, Portugal, in 1962. He received the diploma and doctoral degrees in electronics and telecommunications engineering, from the University of Aveiro, Aveiro, Portugal, in 1985 and 1993, respectively.

From 1985 to 1993, he was an Assistant Lecturer at the University of Aveiro, where, in 1993, he became an Assistant Professor. He is currently an Associate Professor and a Senior Research Scientist in the Telecommunications Institute at the university. His main scientific interests include active device modeling and the analysis and design of various nonlinear microwave and optoelectronics circuits, in particular, the design of highly linear multicarrier power amplifiers and mixers. He has authored or coauthored several papers published in international journals and presented at symposia

Dr. Pedro received the Marconi Young Scientist Award in 1993 and the 2000 Institution of Electrical Engineers, U.K., Measurement Prize. He has served the IEEE as a Reviewer for the IEEE TRANSACTIONS ON MICROWAVE THEORY AND TECHNIQUES and the IEEE MTT-S International Microwave Symposium.